Journal of Applied Physics

Characteristic analysis of coupled microstrip patch resonators on ferrimagnetic substrates

Kunquan Sun, Yinchao Chen, Walter Barry, and John Corlett

Citation: J. Appl. Phys. **79**, 5733 (1996); doi: 10.1063/1.362234
View online: http://dx.doi.org/10.1063/1.362234
View Table of Contents: http://jap.aip.org/resource/1/JAPIAU/v79/i8
Published by the American Institute of Physics.

Characteristic analysis of coupled microstrip patch resonators on ferrimagnetic substrates

Kunquan Sun
Department of Technology, Jackson State University, Jackson, Mississippi 39217

Yinchao Chen
Department of EE, The Hong Kong Polytechnic University, Hong Kong

Walter Barry and John Corlett
Center for Beam Physics, Lawrence Berkeley Laboratory, Berkeley, California 94720

This paper is to use the spectral-domain technique to perform characteristic analysis of coupled microstrip patch resonators on ferrimagnetic substrates. Our formulation has been validated by comparing our result with the published data and showing an excellent agreement between them. Numerical computations have been performed to obtain dependence of resonant frequency on patch dimensions, offset and separation between the two patches, thicknesses of ferrimagnetic film and substrate. It has been seen that as the length of the patch increases the resonant frequency decreases. The larger the offset between the two patches the lower the resonant frequency. The separation between the two patches strongly affects the resonant frequency. It is also found that the resonant frequency increases as the width of the patch decreases. For the fixed dimensions, separation and offset, a thinner substrate results in a higher resonant frequency, and in contrast, a thinner ferrimagnetic film results in a lower resonant frequency.
[S0021-8979(96)75308-8]

I. INTRODUCTION

Recently there is a growing interest[1–4] in microwave integrated circuits (MICs) on ferrimagnetic substrates, especially on epitaxially grown yttrium iron garnet (YIG)/gadolinium gallium garnet (GGG) films due to rapid advances of material technology that makes it possible to contiguously grow and deposit magnetic thin films on different substrates. It is known that a variety of applications of MICs such as filters, oscillators, and tuned amplifiers are directly involved with utilizing microwave resonators.[5] It is the new material technology and demand of MICs on magnetized ferrites that drive investigation of microwave resonators on ferrimagnetic substrates. Great efforts have been made to study microwave resonators with different geometries on YIG/GGG structures.[6,7] It is of our interest in this work to investigate a new configuration of coupled microstrip patch resonators on YIG/GGG with an offset between the two coupled patches as illustrated in Fig. 1.

This paper is to use the spectral-domain technique[8] to study the coupled microstrip patch resonators on YIG/GGG structures. The boundary value problem of the coupled patch resonators is formulated in the spectral domain by the two-dimensional (2D) Fourier-transform. Then Galenkin's method is applied to obtain a system of matrix equations. As a result a secular equation is generated based on the determinant of the system equation and the resonant frequency of the coupled patch resonator can be solved for a given set of dimensions. To assure accuracy of numerical results and efficiency of numerical computations, a set of basis functions is chosen, which accurately represent expected resonant currents on each patch. Numerical computations have been performed. Our results have revealed that resonant frequency depends on patch dimensions, offset and separation between the two patches, and thicknesses of YIG and GGG.

II. FORMULATION

The geometry of the shielded structure of the coupled microstrip patch resonator on YIG/GGG is illustrated in Fig.

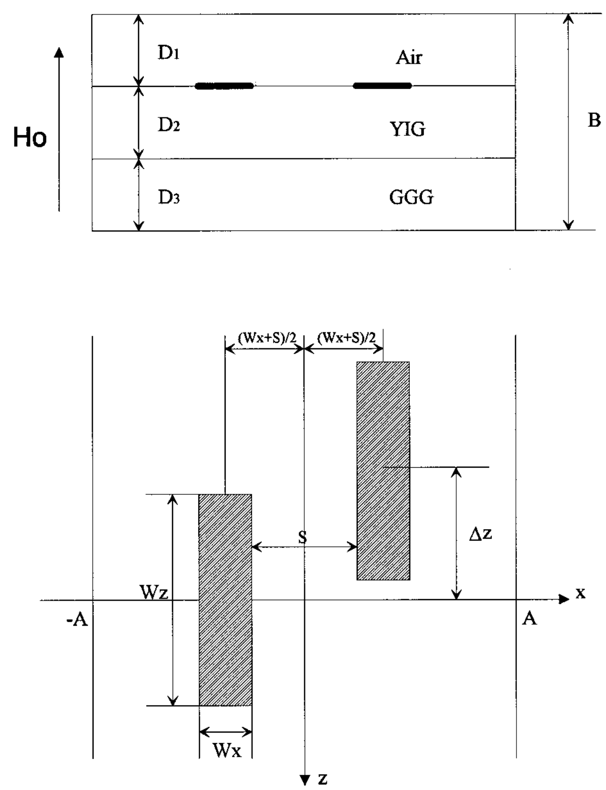

FIG. 1. Cross section and top views of coupled microstrip patch resonator. $2A$ and B the waveguide dimensions, (W_x, W_z) the patch width and length, S the separation between the two patches, Δz the offset between the two patches along the z-axis, and D_1, D_2, and D_3 thicknesses of air region, YIG, and GGG, respectively.

1. Two rectangular patches have dimensions of W_x and W_z, and are separated by a distance of S with an offset of Δz. Thicknesses of YIG and GGG are D_2 and D_3, respectively. A dc magnetic field is applied normal to the plane of YIG film, which is characterized by its static magnetization. Accordingly the permeability tensor of YIG is given as

$$\overleftrightarrow{\mu} = \mu_0 \begin{bmatrix} \mu & 0 & -j\kappa \\ 0 & 1 & 0 \\ j\kappa & 0 & \mu \end{bmatrix} \tag{1}$$

with $\mu = 1 + \omega_h \omega_m / \omega_h^2 - \omega^2$, $\kappa = \omega\omega_m / \omega_h^2 - \omega^2$, where $\omega_h = \gamma\mu_0 H_0$, $\omega_m = \gamma\mu_0 M$, and γ, μ_0, ω, and H_0 are the gyromagnetic ratio, the free-space permeability, the operating frequency, and the internal field, respectively.

In order to formulate the boundary problem in the spectral-domain, the 2D Fourier transforms of every field component and patch currents in xz plane are taken:

$$\tilde{f}(\alpha_n, \gamma, \beta) = \int_{-\infty}^{\infty} \int_{-a}^{a} f(x,y,z) e^{j\alpha_n x + j\beta z} dx dz. \tag{2}$$

In this case summation index n takes on all integer values from minus to plus infinity, since the symmetry of the Green's function is perturbed by the off-diagonal terms in $\overleftrightarrow{\mu}$ of YIG. The above definition of the transform allows the first derivatives with respect to x and z in the space domain to be converted to multiplicative factors in the spectral-domain.

With the transformation defined in Eq. (2) field components of E_x and E_z in YIG film are transformed into the spectral-domain and two coupled equations for $\tilde{E}_x$ and $\tilde{E}_z$ can be obtained to determine the solution to Maxwell's equation. Other field components can be found based on $\tilde{E}_x$ and $\tilde{E}_z$. The electric and magnetic fields in regions of air and GGG can be written as a superposition of TEy and TMy modes.[10] By enforcing the boundary conditions at each of interfaces the Green's function is yielded as follows:

$$\begin{bmatrix} \tilde{E}_z(\alpha_n, \beta) \\ \tilde{E}_x(\alpha_n, \beta) \end{bmatrix} = \begin{bmatrix} \tilde{Z}_{zz}(\alpha_n, \beta) & \tilde{Z}_{zx}(\alpha_n, \beta) \\ \tilde{Z}_{xz}(\alpha_n, \beta) & \tilde{Z}_{xx}(\alpha_n, \beta) \end{bmatrix} \begin{bmatrix} J_z(\alpha_n, \beta) \\ J_x(\alpha_n, \beta) \end{bmatrix}. \tag{3}$$

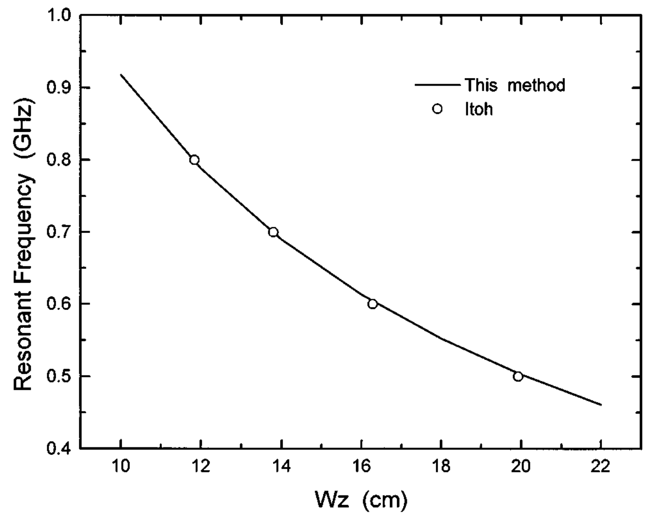

FIG. 2. Resonant frequency vs the patch length W_z with $\epsilon_{xx} = \epsilon_{yy} = \epsilon_{zz} = 2.65$, $D_1 = 8.89$ cm, $D_2 = 1.27$ cm, $D_3 = 0$, $B = 15.5$ cm, and $W_x = 2$ cm.

The remaining task is to employ Galerkin's method along with Paserval's theorem to set up a system equation which includes two sets of homogeneous linear equations. These equations can be solved by setting the determinant of coefficients to zero and searching for the root to find the resonant frequency.

To successfully solve the system equation one must have a proper choice of basis functions that satisfy the edge conditions and have fast convergence properties. In this study the basis functions which are chosen to expand the patch currents are presented below:

$$\begin{aligned} J_x^{(e/o)}(x,z) &= J_x^-(x,z) \mp J_x^+(x,z), \\ J_z^{(e/o)}(x,z) &= J_z^-(x,z) \pm J_z^+(x,z), \end{aligned} \tag{4}$$

with

$$\begin{cases} J_x^-(x,z) = \dfrac{\sin\{(2\pi/W_x)[x + \frac{1}{2}(S+W_x)]\}}{\sqrt{1 - \{(2\pi/W_x)[x + \frac{1}{2}(S+W_x)]\}^2}} \times \dfrac{\sin(\pi z/W_z)}{\sqrt{1-(2z/W_z)^2}}, & -\left(\dfrac{S}{2} + W_x\right) < x < -\dfrac{S}{2} \text{ and } -\dfrac{W_z}{2} < z < \dfrac{W_z}{2} \\ J_x^+(x,z) = \dfrac{\sin\{(2\pi/W_x)[x - \frac{1}{2}(S+W_x)]\}}{\sqrt{1 - \{(2\pi/W_x)[x - \frac{1}{2}(S+W_x)]\}^2}} \times \dfrac{\sin[(\pi/W_z)(z-\Delta z)]}{\sqrt{1-[(2(z-\Delta z)/W_z)]^2}}, & \dfrac{S}{2} < x < \dfrac{S}{2} + W_x \text{ and } \Delta z - \dfrac{W_z}{2} < z < \Delta z + \dfrac{W_z}{2} \end{cases},$$

$$\begin{cases} J_z^-(x,z) = \dfrac{1}{\sqrt{1 - \{(2\pi/W_x)[x + \frac{1}{2}(S+W_x)]\}^2}} \times \dfrac{\cos(\pi z/W_z)}{\sqrt{1-(2z/W_z)^2}}, & -\left(\dfrac{S}{2} + W_x\right) < x < -\dfrac{S}{2} \text{ and } -\dfrac{W_z}{2} < z < \dfrac{W_z}{2} \\ J_z^+(x,z) = \dfrac{1}{\sqrt{1 - \{(2\pi/W_x)[x - \frac{1}{2}(S+W_x)]\}^2}} \times \dfrac{\cos\left[\dfrac{\pi}{W_z}(z-\Delta z)\right]}{\sqrt{1-[2(z-\Delta z)/W_z]^2}}, & \dfrac{S}{2} < x < \dfrac{S}{2} + W_x \text{ and } \Delta z - \dfrac{W_z}{2} < z < \Delta z + \dfrac{W_z}{2} \end{cases},$$

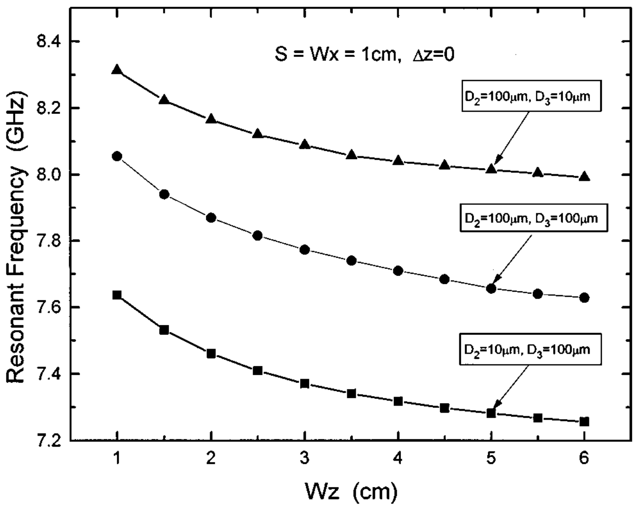

FIG. 3. Dependence of the patch length W_z on resonant frequency as well as impacts of thicknesses of YIG and GGG on resonant frequency.

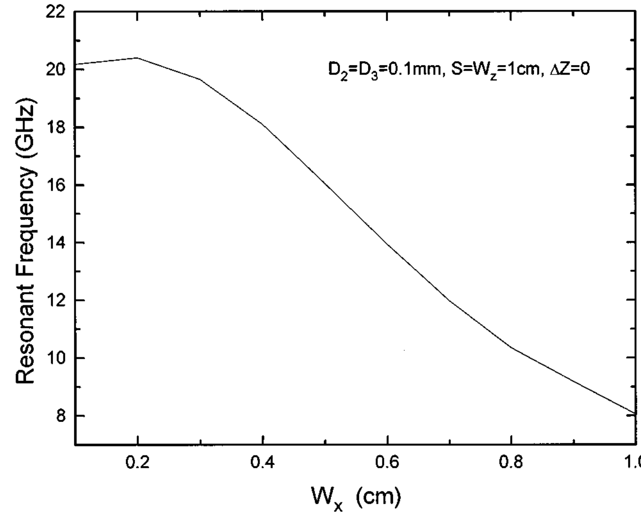

FIG. 5. Resonant frequency vs the patch width W_x.

where the superscription (e/o) denotes even and odd modes, respectively.

III. NUMERICAL RESULTS

In order to validate our formulation and numerical results we simplify the configuration, in which the thickness of GGG is reduced to zero, $S+W_x$ is set to be zero such that the two patches overlap, permeability tensor of YIG is chosen to be that utilized in Ref. 9. Comparison is made between our results and those in Ref. 9 and illustrated in Fig. 2. It is clear that our results agree very well with the published data.

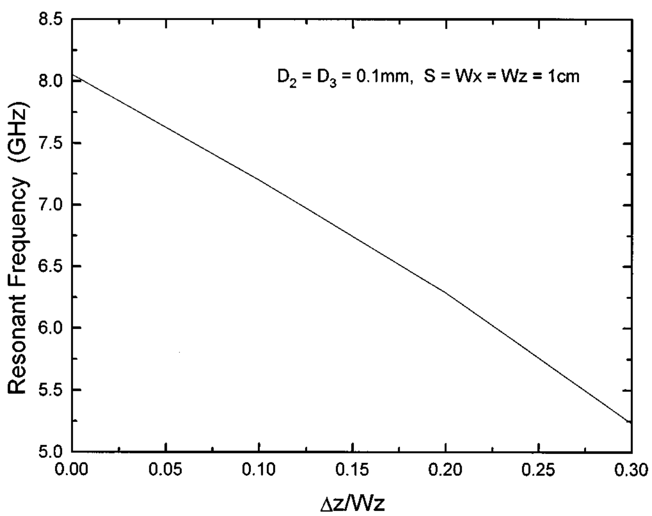

FIG. 4. Resonant frequency vs offset Δz.

Numerical computations have been performed with $\mu_0 H_0 = 0.1T$, $\mu_0 M = 0.175T$, permittivity for YIG and GGG $\epsilon_r = 12.3$, $A = 7.75$ cm and $B = 6$ cm throughout this paper unless stated elsewhere. Both even and odd modes of resonance were calculated. Since there is a slight difference between them, only is the even mode presented in this paper. Figure 3 demonstrates dependence of resonant frequency on the patch length W_z. It is observed that the resonant frequency decreases with W_z. Impacts of thicknesses of YIG and GGG on resonant frequency are illustrated in Fig. 3. For a given set of patch dimensions (W_x, W_z), separation (S) and offset (Δz), a thinner substrate GGG results in a higher resonant frequency, and in contrast, a thinner YIG film results in a lower resonant frequency. Influence of offset between the two patches on resonant frequency was investigated. Figure 4 shows that the resonant frequency decreases with Δz for a given set of (W_x, W_z), S, and thicknesses (D_2 and D_3) of YIG and GGG. Width (W_x) of the resonant patch has the same impact on the resonant frequency as W_z except for $W_x < 0.2$ cm (see Fig. 5). The resonant frequency slightly increase with W_x as W_x is less than 0.2 cm, and then decreases with W_x rapidly.

[1] J. D. Adam, Proc. IEEE **76**, 159 (1988).
[2] D. C. Webb, IEEE Trans. Magn. **24**, 2799 (1988).
[3] E. Schloemann, IEEE Trans. MTT **34**, 1394 (1986).
[4] C. S. Teoh and L. E. Davis, IEEE International Magnetics Conference Digest, April 1995, FD-03.
[5] R. C. Collin, *Foundation for Microwave Engineering* (McGraw-Hill, New York, 1992), Chap. 7.
[6] T. D. Poston and D. D. Stancil, J. Appl. Phys. **53**, (1984).
[7] R. Marcelli, R. Rossi, and P. De Gasperis, IEEE International Magnetics Conference Digest, April 1995, FD-08.
[8] T. Itoh and R. Mittra, IEEE Trans. MTT **21**, 496 (1973).
[9] T. Itoh, IEEE Trans. MTT **22**, 946 (1974).
[10] T. Itoh, *Numerical Techniques for Microwave and Millimeter-Wave Passive Structures* (Wiley, New York, 1989).